frontiers | Frontiers in Materials

TYPE Original Research
PUBLISHED 12 January 2024
DOI 10.3389/fmats.2023.1282919

OPEN ACCESS

EDITED BY
Zhigang Zhang,
Chongqing University, China

REVIEWED BY
Ping Duan,
China University of Geosciences Wuhan, China
Yunchao Tang,
Guangxi University, China

*CORRESPONDENCE
Hui Li,
hla_zyj@qq.com

RECEIVED 25 August 2023
ACCEPTED 22 December 2023
PUBLISHED 12 January 2024

CITATION
Huo G, Jiang X, Sun X, Li H and Shi H (2024), Performance of high-belite calcium sulfoaluminate cement subjected to hydrochloric acid and sulfuric acid. *Front. Mater.* 10:1282919. doi: 10.3389/fmats.2023.1282919

Performance of high-belite calcium sulfoaluminate cement subjected to hydrochloric acid and sulfuric acid

Guang Huo[1,2], Xinchao Jiang[2], Xiaoheng Sun[2], Hui Li[3]* and Hongxing Shi[4]

[1]Shandong Hi-Speed Construction Management Group Co., Ltd., Jinan, China, [2]Shandong Hi-speed Mingdong Expressway Co., Ltd., WeiFang, China, [3]School of Civil and Transportation Engineering, Hebei University of Technology, Tianjin, China, [4]Beijing Zhihuatong Technology Co., LTD., Beijing, China

The high-belite calcium sulfoaluminate cement (HB-CSA) has displayed outstanding acid resistance. However, further research is needed to understand the mechanism behind its acid resistance fully. This study investigates the resistance of a new type of HB-CSA to hydrochloric and sulfuric acid. Additionally, the impact of the ye'elimite ($C_4A_3\bar{S}$)-to-gypsum ($C\bar{S}$) ratio on the acid resistance of HB-CSA is discussed. The resistance performance is investigated by flexural strength and resistance index analyses, X-ray diffraction (XRD), thermogravimetric analysis (TGA), electronic computed tomography (CT) scans, and scanning electron microscopy (SEM). The results show that the HB-CSA exhibits superior resistance to sulfuric acid and hydrochloric acid compared to Portland cement. The absence of portlandite contributes to the enhanced performance of HB-CSA. In addition, as the $C_4A_3\bar{S}$-to-$C\bar{S}$ ratio decreases, the content of Aft in HB-CSA increases, leading to an increase in the acid resistance of HB-CSA.

KEYWORDS

durability, acid attack, high-belite calcium sulfoaluminate cement, ettringite, ye'elimite and gypsum content

1 Introduction

Acid wastewater like domestic wastewater (Congressional budget office, 2002), acid mine drainage (AMD) (Wu et al., 2020a), and cooling towers at power plants (Berndt, 2011) has become a serious global problem due to its adverse impact on the environment and infrastructure (Wu et al., 2020b). As the most widely used structural material, concrete determines the durability of the industrial acidic aqueous treatment (or containment) infrastructure or potentially acid-attack infrastructure (Joorabchian, 2010). However, due to the poor acid corrosion resistance of concrete, repair and reconstruction of acidic aqueous treatment (containment) or acid-attack infrastructure are expensive and time-consuming every year (Congressional budget office, 2002).

The pH of the acid-attack environment usually ranges from 3 to 5 (Larreur-Cayol et al., 2011; Yue et al., 2011; Ninan et al., 2021) or even less than 3 under some special circumstances (Gutiérrez-Padilla et al., 2010). The acid-erosion process of the concrete takes place through a combination of three main mechanisms (Beddoe and Dorner, 2005): 1) the ingress of the acid into the pore solution releases the H^+ ions to decrease the pH in the

TABLE 1 Chemical composition of CSA, HB-CSA-H, HB-CSA-O, and OPC (%).

	SiO_2	Al_2O_3	Fe_2O_3	CaO	MgO	SO_3	TiO_2	LOI	Total
CSA	13.95	22.46	2.67	39.39	2.92	14.34	1.66	1.68	99.07
HB-CSA-H	17.08	15.39	1.37	44.98	4.48	13.80	0.70	1.27	99.05
HB-CSA-O	17.44	15.95	1.35	44.96	4.58	13.04	0.70	1.14	99.16
OPC	23.29	7.47	2.68	55.38	4.22	4.08	0.59	1.8	99.51

TABLE 2 $C_4A_3\bar{S}$-to-$C\bar{S}$ ratio of R-CSA, HB-CSA-H, and HB-CSA-O (-).

	R-CSA	HB-CSA-O	HB-CSA-H
$m(C_4A_3\bar{S})/m\ (C\bar{S})$	2.85	0.92	0.60

TABLE 3 Strength development of HB-CSA, CSA, and OPC mortar specimens with a water-to-cement ratio of 0.5 and a sand-to-cement ratio of 2.5 (MPa).

	Flexural strength/compressive strength		
	1 day	7 days	28 days
R-CSA	9.1/39.1	9.5/53.2	9.5/56.0
HB-CSA-O	7.0/37.6	8.0/50.9	8.3/65.0
HB-CSA-H	7.2/36.4	7.8/44.2	7.8/50.3
OPC	3.5/12.1	6.7/36.7	10.7/51.8

pore solution; 2) the free OH^- and alkali in the pore solution are progressively consumed by neutralizing the H^+ ions, reducing the pH of the pore solution and increasing the dissolution of portlandite from the matrix; and 3) C-S-H starts dissolving due to the reduction in pH. In addition, when the concrete made using ordinary Portland cement (OPC) is exposed to a sulfuric acid environment, the dissolution of CH occurs followed by the formation of gypsum ($CaSO_4{\cdot}2H_2O$). This process introduces further damage due to sulfate attack, i.e., expansion due to ettringite formation and subsequent cracking, as reported by Beddoe (2016). Following this, data suggest that the chemical erosion rates of sulfuric acid are faster than those of hydrochloric acid and nitric acid (Bassuoni and Nehdi, 2007). The corrosion of hydration products in the concrete makes the structures looser, reducing the strength and impermeability of concrete, representing a potentially major safety hazard and durability issues (Girardi et al., 2010). Studies on concrete to increase the resistance to acid attack have focused on decreasing the ratio of water to cement (w/c) to make the mortar denser (Kim et al., 2014) and mixing supplementary cementing materials (SCMs), such as fly ash (FA), granulated blast furnace slag (GBFS), and silica fume (SF), to decrease the alkalinity of concrete (Mlinárik and Kopecskó, 2017). However, these methods have little effect on improving the acid resistance since ordinary Portland cement, the most widely used in civil engineering, has poor resistance to acid corrosion (Imbabi et al., 2012; Xu et al., 2017; Maddalena et al., 2018).

Recently, calcium sulfoaluminate (CSA) cement has emerged as an alternative cementing material owing to its advantages, such as low carbon emissions (Glasser and Zhang, 2001; Gartner, 2004), rapid hardening (Hou et al., 2020), and excellent performance in acid environments (Dyer, 2017; Gartner and Sui, 2018; Yang et al., 2018). Although CSA has many advantages, it has obvious shortcomings. The manufacturing of CSA strongly depends on the high quality of bauxite (Chaunsali and Mondal, 2015), which limits large-scale production. In addition, mechanical properties such as the compressive strength and flexural strength of concrete made using CSA may be reduced after long-term aging because of the expansion caused by the production of a large amount of ettringite ($3CaO{\cdot}Al_2O_3{\cdot}3CaSO_4{\cdot}32H_2O$, AFt) (Ogawa and Roy, 1982; Zhang, 2015). To overcome the shortcomings of CSA, a promising alternative with the rapid setting and hardening of high-belite calcium sulfoaluminate (HB-CSA) cement has been developed (Li et al., 2014). The HB-CSA clinker is mainly composed of ye'elimite ($3CaO{\cdot}3Al_2O_3{\cdot}CaSO_4$, $C_4A_3\bar{S}$) and belite ($2CaO{\cdot}SiO_2$, C_2S), and the strength of HB-CSA would not decrease at late ages owing to its increased C_2S content (Wang et al., 2022). However, since the content of $C_4A_3\bar{S}$ decreases, the early and final strength of HB-CSA is lower than that of CSA (Chi et al., 2021). By adjusting the amount of gypsum and mineral admixtures in cement, the early and final strength of HB-CSA has been significantly increased, and a new type of HB-CSA has been proposed (Zhang et al., 2022). The new type of HB-CSA has been successfully used as a repair material, flooring material, and UHPC. It was also used as the activator to increase the blast slag activity and proposed a high-performance cement named calcium sulfoaluminate-activated supersulfated cement (CSA-SSC) (Sun et al., 2022). Since HB-CSA is a type of CSA, HB-CSA is expected to be an ideal material for acidic aqueous treatment (containment) infrastructure. However, because the mineral content of HB-CSA differs somewhat from that of conventional CSA, particularly in terms of the mass ratio of $C_4A_3\bar{S}$-to-$C\bar{S}$, the acid corrosion resistance of HB-CSA must differ from that of CSA.

This study aims to investigate changes in the chemical components and mechanical evolution of the new type of HB-CSA when exposed to the hydrochloric and sulfuric acid solutions and understand the underlying mechanisms of their evolution under such exposure conditions. Specimens were evaluated based on their changes in flexural strength, composition, and microstructure under the coupling effect of sulfuric acid and sulfuric acid attacks. The influence of the mass ratio of $C_4A_3\bar{S}$ to $C\bar{S}$ on the acid corrosion resistance capability of CSA was also discussed.

10.3389/fmats.2023.1282919

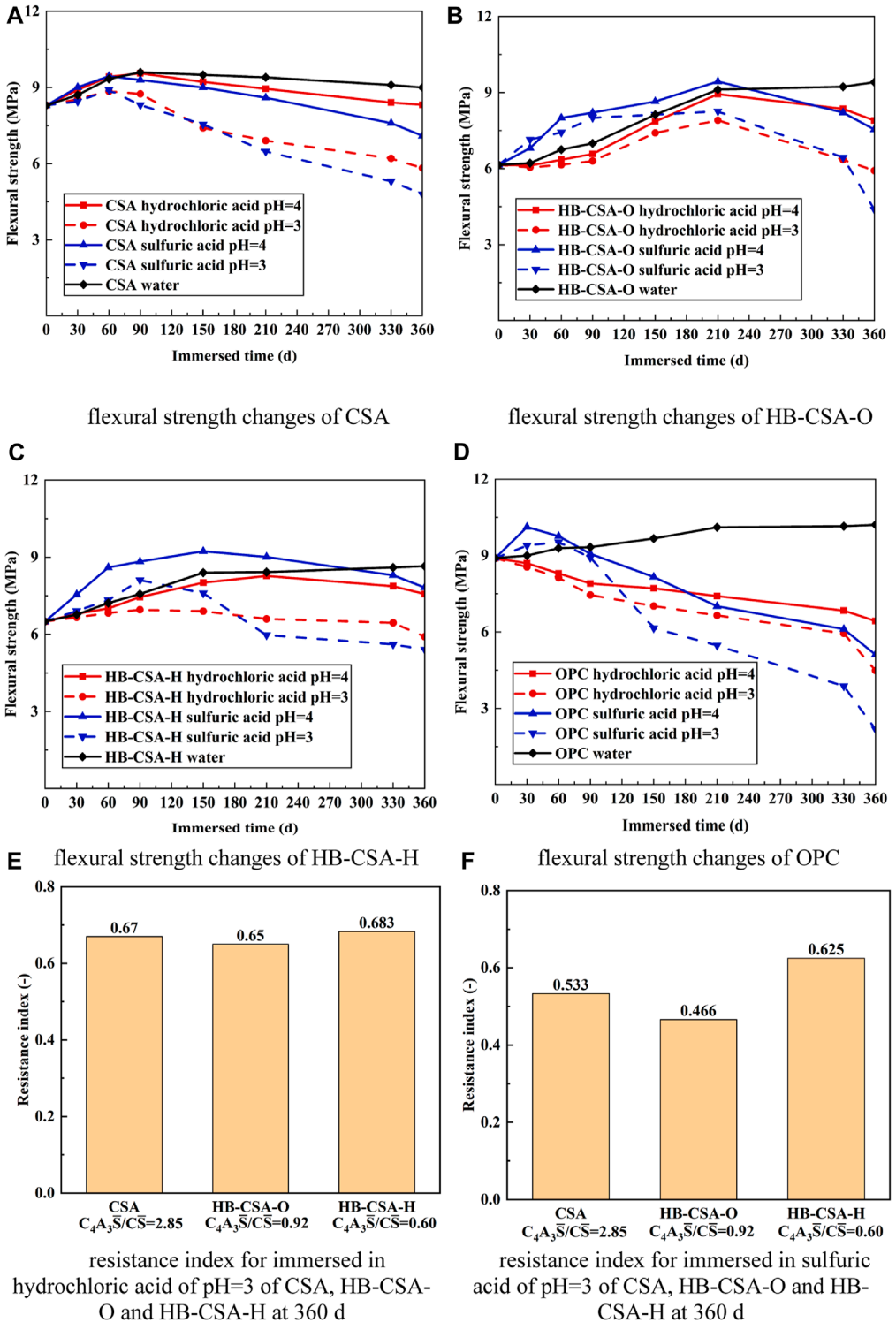

FIGURE 1
Flexural strength changes and resistance indexes of CSA, HB-CSA-O, HB-CSA-H, and OPC immersed in different acid solutions. **(A)** Flexural strength changes in CSA, **(B)** flexural strength changes in HB-CSA-O, **(C)** flexural strength changes in HB-CSA-H, **(D)** flexural strength changes in OPC, **(E)** resistance indexes of CSA, HB-CSA-O, and HB-CSA-H immersed in hydrochloric acid at pH 3 for 360 days, and **(F)** resistance indexes of CSA, HB-CSA-O, and HB-CSA-H immersed in sulfuric acid at pH 3 for 360 days.

10.3389/fmats.2023.1282919

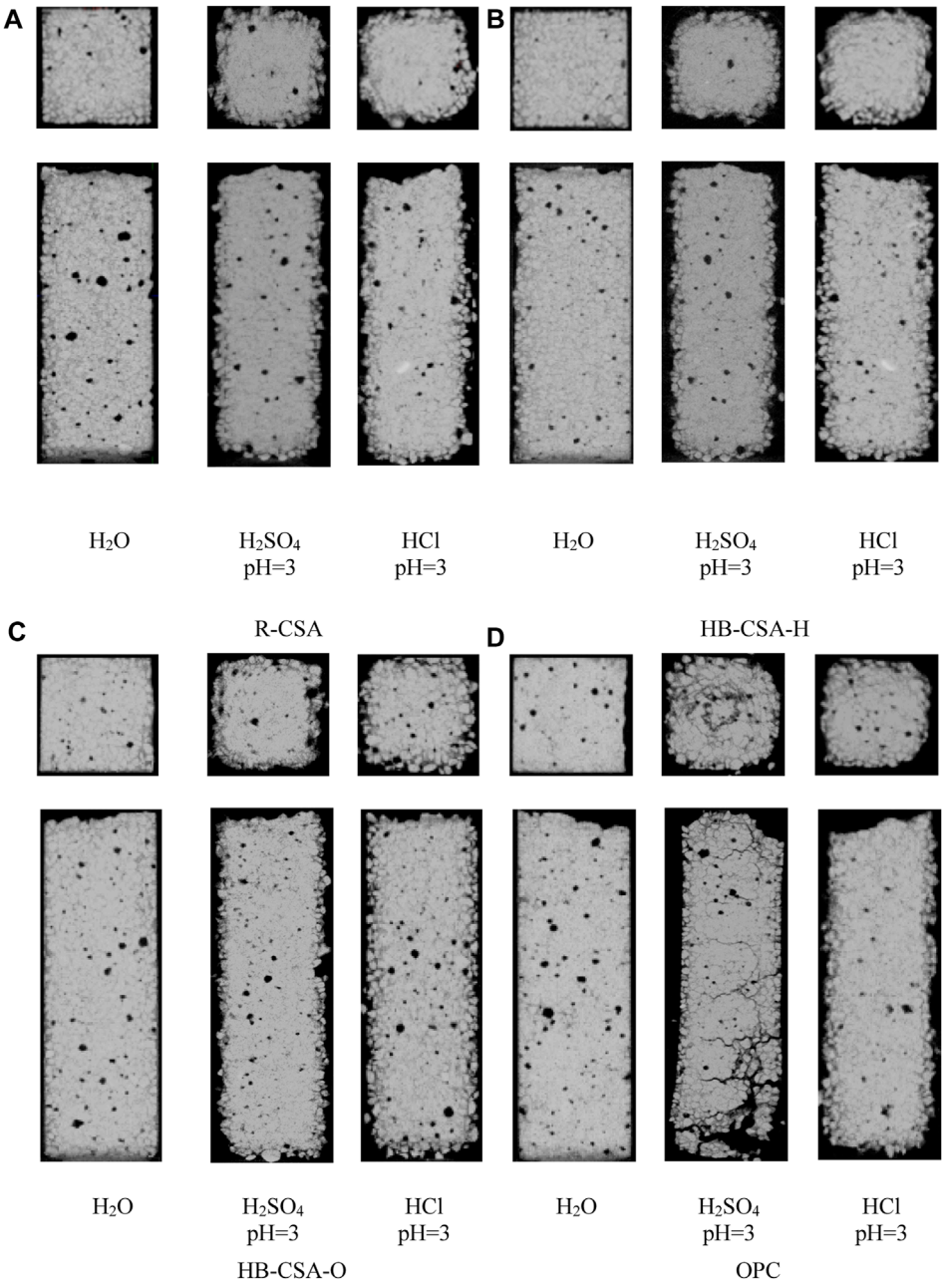

FIGURE 2
Structure morphology obtained by CT for mortar specimens exposed to water, hydrochloric acid solution, and sulfuric acid solution at pH 3 for 360 days. **(A)** R-CSA, **(B)** HB-CSA-H, **(C)** HB-CSA-O, and **(D)** OPC.

2 Experimental

2.1 Materials

OPC, CSA, and HB-CSA were used in this research. OPC was prepared using 42.5 R Portland cement (a Chinese cement standard with a 28-day compressive strength of at least 42.5 MPa obtained based on the given ratio). Two types of HB-CSA, namely, HB-CSA-H and HB-CSA-O, were used in this study to investigate the influence of the mass ratio of $C_4A_3\overline{S}$ to $C\overline{S}$ on the acid resistance behavior of HB-CSA. Table 1 shows the chemical compositions of CSA, HB-CSA-H, HB-CSA-O, and OPC. Table 2 shows the mass ratio of $C_4A_3\overline{S}$ to $C\overline{S}$ for CSA, HB-CSA-H, and HB-CSA-O. It is worth noting that the mass ratio of $C_4A_3\overline{S}$ to $C\overline{S}$ in HB-CSA-O is higher than that in HB-CSA-H. This suggests that the content of $C_4A_3\overline{S}$ is more in HB-CSA-O relative to $C\overline{S}$. The fine aggregate was natural sand of 0–6 mm in diameter and crushed stone dust of 0–6 mm in diameter, with a fineness modulus of 2.5.

The hydrochloric and sulfuric acid solutions were diluted with pure water to obtain the required pH. The hydrochloric

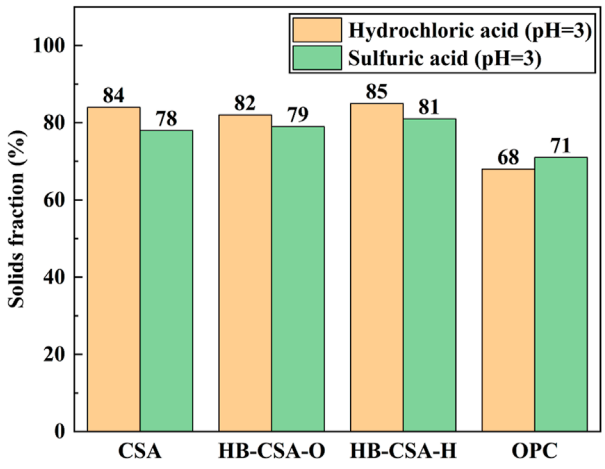

FIGURE 3
Solid fractions of CSA, HB-CSA-O, HB-CSA-H, and OPC immersed in acid at pH 3 for 360 d.

acid solutions with pH 3 and 4 were prepared as the corrosive solutions since the pH of acid wastewater is usually in the range of 3–5 in acidic aqueous treatment (containment) infrastructure (Larreur-Cayol et al., 2011; Yue et al., 2011; Ninan et al., 2021). In addition, the sulfuric acid solutions with pH 4 and 3 were prepared to investigate the chemical components and mechanical evolution of HB-CSA under the coupling effect of acid and sulfate attacks.

2.2 Mix proportion and sample preparation

HB-CSA (HB-CSA-H and HB-CSA-O), CSA, and OPC mortar specimens with a water–cement ratio of 0.5 and sand–cement ratio of 2.5 were prepared using the following procedure: first, water, sand, and cement were combined in a mixer and then stirred for 3 min. After stirring, the mortar was poured into metal molds of dimensions 10 mm × 10 mm × 60 mm. The mortar with molds was cured at a temperature of 20°C and relative humidity of 95% for 24 h. All the specimens were then de-molded and cured in water at a temperature of 20°C for another 27 days.

Plastic containers sealed with lids were used to hold the specimens and corrosive solutions. Each container contained 27 samples and 6 L of acid solution. Meanwhile, samples soaked in water of the same volume were set as the control group. All the containers were maintained at 20°C. A handheld pH meter was used to detect the acidity of the corrosive solutions at regular intervals, and the hydrochloric and sulfuric acid solutions were restored when the pH of the solution increased by 0.5.

2.3 Test methods

The strength development of HB-CSA and OPC mortar during curing was measured according to the Chinese standard GB/T 17671-2021 (ISO679:2009) and is listed in Table 3. The changes in flexural strength, chemical components, and structural morphology of each type were measured after the specimens were immersed in different acid solutions for 30, 60, 90, 120, 150, 210, 330, and 360 days.

As a non-destructive testing method, CT can quickly obtain the realistic internal structure of the specimen after acid erosion for the qualitative characterization of the acid erosion damage degree of the specimen. At the same time, the images obtained by CT can be processed using image processing technology (Li et al., 2022) or computer deep learning (Wu et al., 2003; Que et al., 2023) to quantitatively analyze the width and other related parameters of the cracks and quantitatively evaluate the damage degree of the specimen. In this study, a YXLON FF35 electronic computed tomography (CT) scanner was used for the visual inspection of the specimens before and after being immersed in different acid solutions for different immersion times. The current and voltage used in this test were 120 kV and 200 μA, respectively. The step size was 0.11°, and a two-frame averaging technique was used to form the images.

The average flexural strength of specimens with different immersion times was measured following the three-point bending experiment. The test is performed under load control at a constant rate of 0.78 N/s, and nine specimens were tested per group in this test. The maximum and minimum values were discarded, and the average of the remaining seven values was taken as the test result. The percentage change in flexural strength was also calculated by the strength change between the specimens immersed in acid solutions and water. The percentage change is denoted as the resistance index (K) and can be expressed using Eq. 1 according to the Chinese standard GB/T 50082-2009.

$$K = \frac{F_s}{F_w}, \tag{1}$$

where F_s is the flexural strength of a specimen immersed in acid solutions and F_w is the flexural strength of a specimen immersed in water.

After flexural strength testing, the undamaged part of the specimens was broken into small pieces for chemical and microscopic tests. X-ray diffraction (XRD) was used to analyze the hydration and corrosion products of HB-CSA (HB-CSA-H and HB-CSA-O), CSA, and OPC at the selected ages. Dried samples were ground into a powder with a size of less than 60 μm. The current and voltage of the Bruker D8 Advance 1,600 W instrument were 40 kV and 40 mA, respectively. The radiation source used was Cu-Kα radiation, and the 2θ ranged from 5° to 70°. The step size was 0.01°, and each step took 0.2 s.

Thermogravimetric analysis (TGA) was also used along with XRD to analyze the hydration and corrosion products. A Mettler Toledo TGA/DSC-1600 instrument was used in this test. The ground samples (less than 60 μm) were placed in Al_2O_3 crucibles and heated from 30°C to 600°C with a 10 K/min heating rate in a nitrogen atmosphere.

Image analysis based on scanning electron microscopy (SEM) is used to analyze visual changes in morphology before and after the acid attack. A cross section of the sample was selected for observation. Crushed samples with a size of approximately 5 mm were selected, and gold spray was applied prior to the test to improve

10.3389/fmats.2023.1282919

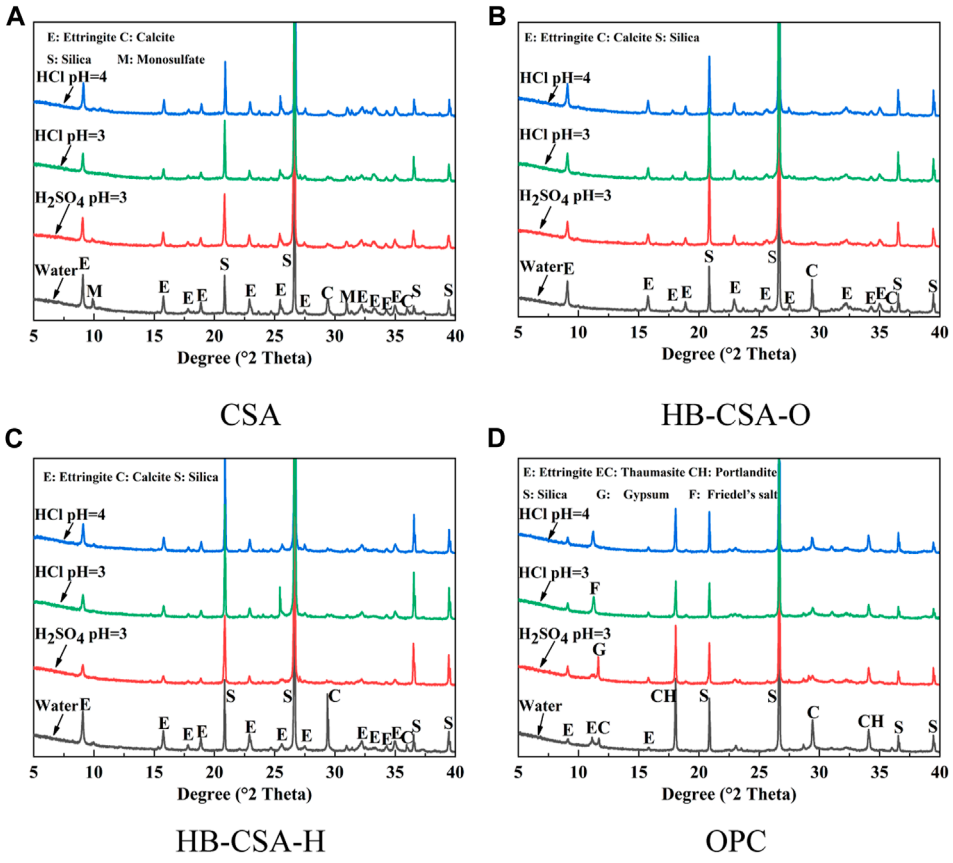

FIGURE 4
XRD patterns of CSA, HB-CSA, and OPC specimens after being immersed in hydrochloric acid at pH 3 and 4 and sulfuric acid at pH 3 for 360 days. **(A)** CSA, **(B)** HB-CSA-O, **(C)** HB-CSA-H, and **(D)** OPC.

the conductivity. A Nova NanoSEM 450 microscope was used, and the voltage was 10 kV.

3 Results and discussion

3.1 Flexural strength evolution

Figure 1 displays the flexural strength changes observed in the specimens immersed in various acid solutions for different immersion times. For specimens immersed in water, the flexural strength of CSA reaches the peak at 90 days and slightly decreases after reaching the peak. The maximum flexural strength of CSA is 9.6 MPa and falls to 9.0 MPa at 360 days of immersion in water. The flexural strength of HB-CSA-H gradually increases as the immersion time increases, reaching stability (approximate peak) after being immersed in water for 360 days. Specifically, the flexural strength of HB-CSA-H increases from 6.50 to 8.65 MPa when the specimens are immersed in water for 360 days. For HB-CSA-O, the trend of flexural strength change in HB-CSA-O is similar to that in HB-CSA-H. However, the early strength of HB-CSA-O (6.15 MPa after 0 days of immersion) is lower than that of HB-CSA-H. On the other hand, the long-term strength of HB-CSA-O (9.41 MPa after 360 days of immersion) is higher than that of HB-CSA-H. The strength increase in HB-CAS-O and HB-CSA-H in the long term may be attributed to the hydration of belite in cement. For OPC, the flexural strength development trends gently after being immersed in water for 360 days. The maximum flexural strength is approximately 10.10 MPa.

When the specimens are immersed in hydrochloric acid, the flexural strength of CSA, HB-CSA-O, and HB-CSA-H show a similar change trend of an increase followed by a decrease in flexural strength. In contrast, the flexural strength of OPC mortar specimens immersed in hydrochloric acid always decreases with the increase in immersion time. Differences in peak flexural strength arrival timing were observed in CSA, HB-CSA-O, and HB-CSA-H. CSA reaches its peak flexural strength after being immersed in hydrochloric acid for 60 days at pH 4 and 3. HB-CSA-O reaches its peak flexural strength after being immersed in hydrochloric acid for 210 days at pH 4 (or 90 days at pH 3), while HB-CSA-H reaches its peak flexural strength after being immersed in hydrochloric acid for 150 days at pH 4 (or 90 days at pH = 3). Based on the test results, it is indicated that CSA, HB-CSA-O, and HB-CSA-H exhibit strong resistance to hydrochloric acid corrosion. Even after being immersed in hydrochloric acid with a pH of 4 for 360 days, the flexural strength of CSA, HB-CSA-O, and HB-CSA-H remains stable at 8.32, 7.57, and 7.9 MPa, respectively. Similarly, after being immersed in hydrochloric acid with a pH of 3 for 360 days, the flexural

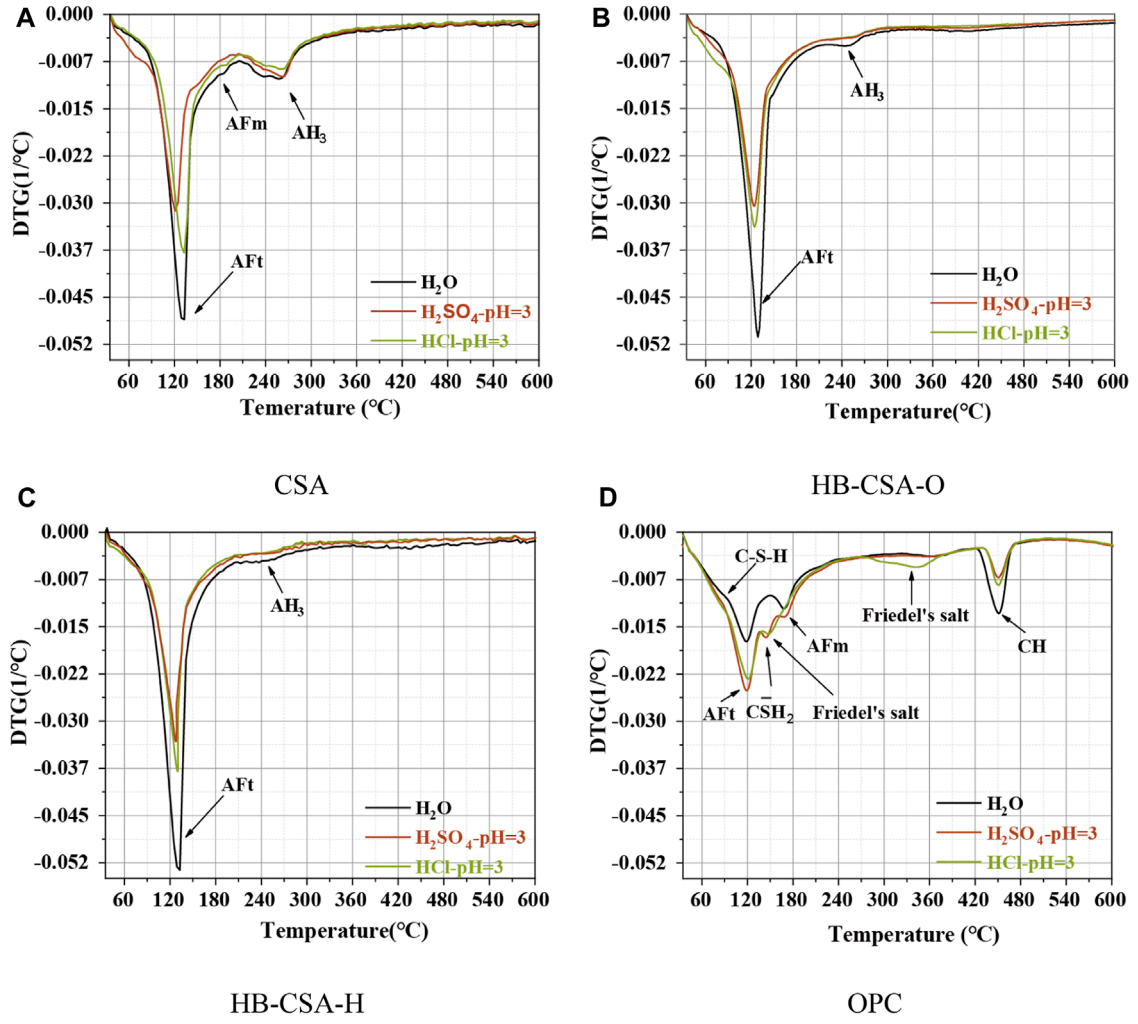

FIGURE 5
DTG patterns of CSA, HB-CSA, and OPC specimens after being immersed in hydrochloric acid and sulfuric acid at pH 3 for 360 days. **(A)** CSA, **(B)** HB-CSA-O, **(C)** HB-CSA-H, and **(D)** OPC.

strength of CSA, HB-CSA-O, and HB-CSA-H remains consistent at 6.02, 5.91, and 5.92 MPa, and the corresponding resistance indexes of CSA, HB-CSA-O, and HB-CSA-H remain 0.670, 0.650, and 0.683, respectively. It is found that the ability of hydrochloric acid corrosion resistance of HB-CSA increases with a decrease in the $C_4A_3\overline{S}$-to-$C\overline{S}$ ratio. After being immersed in hydrochloric acid, the flexural strength of OPC decreases significantly. Specifically, its strength drops from 8.9 to 6.43 MPa after being immersed in hydrochloric acid with a pH of 4 for 360 days and falls from 8.9 to 4.49 MPa after being immersed in hydrochloric acid with a pH of 3 for 360 days.

When immersed in sulfuric acid, the flexural strength of CSA, HB-CSA-O, HB-CSA-H, and OPC experiences an increase in the early stage of immersion. During this stage, the flexural strength of these cement specimens immersed in sulfuric acid is greater than that of the specimens immersed in water for the same time of immersion (except CSA immersed in pH 3 of sulfuric acid). Particularly, for HB-CSA-O and HB-CSA-H, the flexural strength increases notably until 210 days and 150 days of immersion, respectively. However, after reaching the peak of flexural strength, the fall in flexural strength of specimens immersed in sulfuric acid is much faster than that of the specimens immersed in hydrochloric acid. As a result, specimens immersed in sulfuric acid for 360 days have lower flexural strength compared to those immersed in hydrochloric acid with the same pH and immersion time. The resistance indexes of CSA, HB-CSA-O, and HB-CSA-H remain 0.533, 0.466, and 0.625 for specimens immersed in sulfuric acid with a pH of 3 at 360 days. It can be found that the ability of sulfuric acid corrosion resistance of HB-CSA increases with a decrease in the $C_4A_3\overline{S}$-to-$C\overline{S}$ ratio. When OPC is immersed in sulfuric acid, its flexural strength decreases significantly compared to other types of cement. After being immersed in sulfuric acid with a pH of 4 for 360 days, its flexural strength decreases from 8.9 to 5.11 MPa. Similarly, when immersed in sulfuric acid with a pH of 3 for 360 days, its flexural strength drops further to 2.18 MPa.

10.3389/fmats.2023.1282919

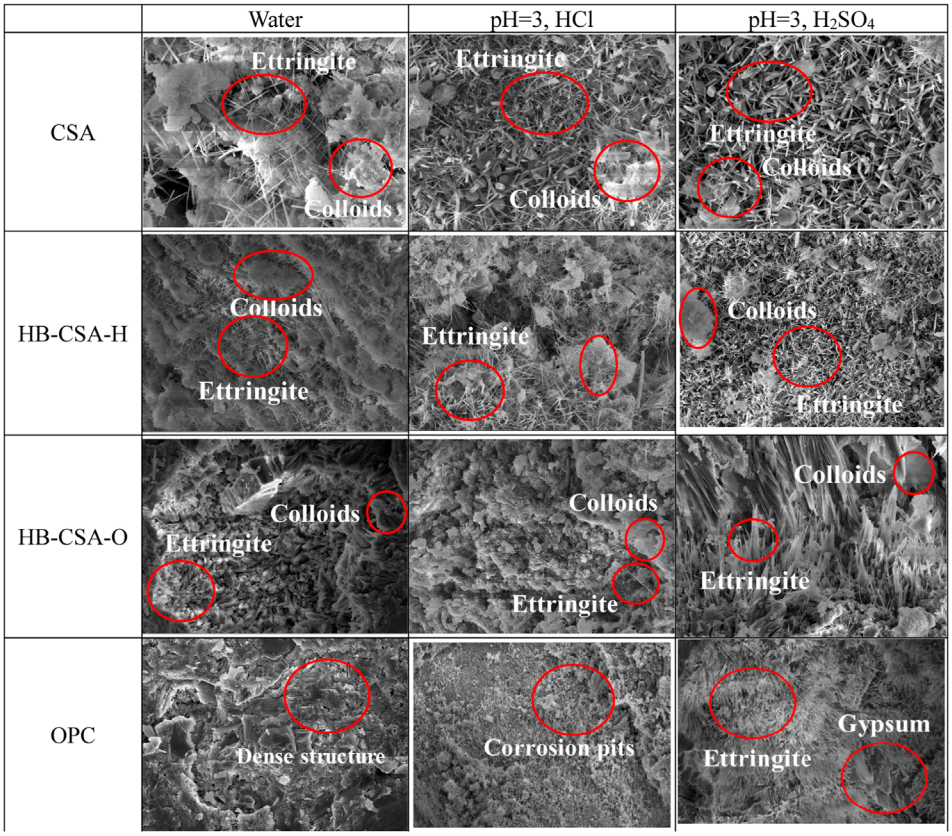

FIGURE 6
SEM images of specimens immersed in water, hydrochloric acid, and sulfuric acid for 360 days.

3.2 Internal structure changing

Figure 2 displays the internal structure morphology obtained by CT for specimens immersed in water, hydrochloric acid solution at pH 3, and sulfuric acid solution at pH 3 for 360 days. The color and density of the samples as shown in the figure positively correlate with the results of CT. Brighter and whiter colors correspond to the matrix, and the black color corresponds to the pores, corrosion pits, and cracks. For CSA and HB-CSA, the corrosion pits and micro-cracks appeared on the surface of the specimens after being immersed in the hydrochloric acid and sulfuric acid solutions at pH 3 for 360 days, which increased the surface roughness of the specimens. However, the morphological integrity in the core of the specimen was well maintained. For OPC mortar specimens, corrosion becomes more severe. Particularly, in the sulfuric acid corrosion, big cracks form on the surface of the specimen and extend into the core of the specimen, which damages the structure of the matrix.

The solid fractions of specimens immersed in hydrochloric acid and sulfuric acid for 360 days are obtained by calculating the brighter and whiter areas in CT images and summarized in Figure 3. The loss of flexural strength in CSA, HB-CSA-O, and HB-CSA-H when immersed in sulfuric and hydrochloric acid solutions is directly related to the reduction in their solid fraction, as observed from the specimens' solid fraction combined with their flexural strength test results. The more the solid loss, the more severe the strength loss. In the case of CSA, HB-CSA-O, and HB-CSA-H, the solid fraction of specimens immersed in hydrochloric acid for 360 days is greater than that of the specimens immersed in sulfuric acid. Therefore, the corresponding flexural strength of specimens immersed in hydrochloric acid is higher than that of the specimens immersed in sulfuric acid with the same pH and immersion time. For OPC, serious cracks tend to form in the specimen immersed in sulfuric acid. As a result, the flexural strength of OPC immersed in sulfuric acid for 360 days is significantly lower than that of the specimens immersed in hydrochloric acid with the same pH and immersion time.

3.3 Changes in microstructure and mineralogy

Figures 4, 5 show the results of XRD and differential thermal analysis (DTG) of specimens immersed in water, hydrochloric acid solution at pH 3 and 4, and sulfuric acid solution at pH 3 for 360 days. For CSA, the main hydration product is AFt. Since gypsum is insufficient to convert all minerals into AFt, some monosulfate (AFm) and alumina gel (AH) are found in the hydration of CSA. In the case of HB-CSA-O and HB-CSA-H, AFt is also the primary product of hydration. However, due to the ample content of gypsum in cement, no AFm is detected in the hydration products. Only a

minimal amount of AH is found. In addition, some calcium silicate hydrates are found since HB-CSA-H and HB-CSA-O contain a certain amount of C_2S. For HB-CSA-H, the content of AFt is higher than that of HB-CSA-O since the gypsum content in HB-CSA-H is higher than that in HB-CSA-O, resulting in the conversion of AH to AFt. Meanwhile, the content of AH in HB-CSA-H is lower than that in HB-CSA-O. No new products are generated during the corrosion process of CSA, HB-CSA-H, and HB-CSA-O in hydrochloric acid and sulfuric acid. The strength loss of these three types of cement can be attributed to the dissolution of the hydration products. Specimens immersed in sulfuric acid have their hydration products more dissolved than those immersed in hydrochloric acid, ultimately resulting in lower flexural strength. For CSA, the acid corrosion causes a large amount of dissolution of AFt and AFm, but the amount of AH dissolved in CSA is minimal. For HB-CSA-H and HB-CSA-O, in addition to the dissolution of AFt, AH also has a certain amount of dissolution. After 360 days of acid corrosion, the residual content of AFt in HB-CSA-H is higher than that in CSA and HB-CSA-O. Due to this, the flexural strength of the HB-CSA-H specimen immersed in acid is higher than that of the other two types of cement with the same immersion time in acid. For OPC, new hydration products are generated along with the acid corrosion, i.e., Friedel's salt for hydrochloric acid corrosion and AFt and gypsum for sulfuric acid corrosion. The expansion of gypsum causes cracking and damage to OPC specimens immersed in sulfuric acid.

SEM images (×3,000 magnification) of mortar specimens immersed in water, hydrochloric acid solution at pH 3, and sulfuric acid solution at pH 3 for 360 days are shown in Figure 6. For OPC mortar specimens, a dense structure consisting of C-S-H is formed in the specimens immersed in water for 360 days. After being corroded by hydrochloric acid and sulfuric acid, the matrix becomes looser and much fibrous product occurs in the specimen immersed in sulfuric acid. Based on the experimental results of TGA, it can be concluded that the fibrous products formed are ettringite and gypsum crystals for OPC immersed in sulfuric acid. The looser structure of OPC immersed in sulfuric acid can be attributed to the production of large-sized gypsum crystals, which cause structural expansion and cracking leading to a decrease in flexural strength. As observed in SEM images, the microstructure of CSA, HB-CSA-H, and HB-CSA-O appears similar when immersed in either hydrochloric acid or sulfuric acid. The only discernible differences are in the size of AFt and the amount of colloidal hydration products. The content of colloidal products in specimens immersed in hydrochloric acid is higher than that in specimens immersed in sulfuric acid. This causes a reduction in the flexural strength of specimens immersed in sulfuric acid compared to those immersed in hydrochloric acid.

4 Conclusion

This study aims to investigate the changes in the chemical components and mechanical evolution of HB-CSA when exposed to sulfuric and hydrochloric acid solutions and understand the underlying mechanisms of their evolution under such exposure conditions. In addition, the influence of the mass ratio of $C_4A_3\overline{S}$ to $C\overline{S}$ on the acid corrosion resistance capability of HB-CSA is also discussed. The following conclusions are drawn:

(1) HB-CSA exhibits superior resistance to sulfuric acid and hydrochloric acid compared to OPC. When the specimens are immersed in hydrochloric acid at a pH of 3 for 360 days, the flexural strength of HB-CSA-O and HB-CSA-H remains 5.91 and 5.92 MPa, respectively. At the same time, the flexural strength of OPC remains only 4.49 MPa. The same results are obtained in the sulfuric acid-corroded specimens.

(2) No new products are generated during the corrosion process of HB-CSA in hydrochloric and sulfuric acid solutions. The strength loss of HB-CSA can be attributed to the dissolution of the hydration products. The HB-CSA specimens immersed in sulfuric acid have a greater dissolution amount of hydration product than those immersed in hydrochloric acid, resulting in lower flexural strength than those immersed in hydrochloric acid.

(3) As the $C_4A_3\overline{S}$-to-$C\overline{S}$ ratio in HB-CSA decreases, the amount of AFt present in HB-CSA increases. AFt has excellent resistance to acid attack, and thus, after being immersed in a certain acid solution for 360 days, the residual content of AFt present in HB-CSA with a lower $C_4A_3\overline{S}$-to-$C\overline{S}$ ratio is greater than that in HB-CSA with a higher $C_4A_3\overline{S}$-to-$C\overline{S}$ ratio. Consequently, after being immersed in a certain acid solution for 360 days, the flexural strength of the HB-CSA specimen with a lower $C_4A_3\overline{S}$-to-$C\overline{S}$ ratio is higher than that of the HB-CSA specimen with a higher $C_4A_3\overline{S}$-to-$C\overline{S}$ ratio.

Data availability statement

The original contributions presented in the study are included in the article/Supplementary Material; further inquiries can be directed to the corresponding author.

Author contributions

GH: data curation and writing–original draft. XJ: investigation, methodology, and writing–original draft. XS: investigation and writing–review and editing. HL: conceptualization and writing–original draft. HS: investigation, methodology, and writing–review and editing.

Funding

The author(s) declare that financial support was received for the research, authorship, and/or publication of this article. This study was financially supported by the National Natural Science Foundation of China (No. 52008150) and the Natural Science Foundation of Hebei Province, China (No. E2021202037).

Acknowledgments

The authors would like to acknowledge the financial support provided by the National Natural Science Foundation of China

(No. 51702082), the Natural Science Foundation of Hebei Province, China (No. E2021202037), and Tangshan Polar Bear Building Materials Co., Ltd., Tangshan, China.

Conflict of interest

Author GH was employed by Shandong Hi-Speed Construction Management Group Co., Ltd., and Shandong Hi-speed Mingdong Expressway Co., Ltd. Authors XJ and XS were employed by Shandong Expressway Mingdong Highway Co., Ltd. Author HS was employed by Beijing Zhihuatong Technology Co., Ltd.

The remaining author declares that the research was conducted in the absence of any commercial or financial relationships that could be construed as a potential conflict of interest.

Publisher's note

All claims expressed in this article are solely those of the authors and do not necessarily represent those of their affiliated organizations, or those of the publisher, the editors, and the reviewers. Any product that may be evaluated in this article, or claim that may be made by its manufacturer, is not guaranteed or endorsed by the publisher.

References

Bassuoni, M. T. T., and Nehdi, M. L. L. (2007). Resistance of self-consolidating concrete to sulfuric acid attack with consecutive pH reduction. *Cem. Concr. Res.* 37, 1070–1084. doi:10.1016/j.cemconres.2007.04.014

Beddoe, R. E. (2016). Modelling acid attack on concrete: part II. A computer model. *Cem. Concr. Res.* 88, 20–35. doi:10.1016/j.cemconres.2015.10.012

Beddoe, R. E., and Dorner, H. W. (2005). Modelling acid attack on concrete: part I. The essential mechanisms. *Cem. Concr. Res.* 35, 2333–2339. doi:10.1016/j.cemconres.2005.04.002

Berndt, M. L. (2011). Evaluation of coatings, mortars and mix design for protection of concrete against sulphur oxidising bacteria. *Constr. Build. Mater.* 25 (10), 3893–3902. doi:10.1016/j.conbuildmat.2011.04.014

Chaunsali, P., and Mondal, P. (2015). Influence of calcium sulfoaluminate (CSA) cement content on expansion and hydration behavior of various ordinary portland cement-CSA blends. *J. Am. Ceram. Soc.* 98 (8), 2617–2624. doi:10.1111/jace.13645

Chi, L., Wang, Z., Lu, S., Wang, H., Liu, K., and Liu, W. (2021). Early assessment of hydration and microstructure evolution of belite-calcium sulfoaluminate cement pastes by electrical impedance spectroscopy. *Electrochimica Acta* 389, 138699. doi:10.1016/j.electacta.2021.138699

Congressional budget office (2002). *Future investment in drinking and wastewater infrastructure*. Washington, DC: Congressional Budget Office. ISBN 0160512433.

Dyer, T. (2017). Influence of cement type on resistance to attack from two carboxylic acids. *Cem. Concr. Compos.* 83, 20–35. doi:10.1016/j.cemconcomp.2017.07.004

Gartner, E. (2004). Industrially interesting approaches to "low-CO_2" cements. *Cem. Concr. Res.* 34, 1489–1498. doi:10.1016/j.cemconres.2004.01.021

Gartner, E., and Sui, T. B. (2018). Alternative cement clinkers. *Cem. Concr. Res.* 114, 27–39. doi:10.1016/j.cemconres.2017.02.002

Girardi, F., Vaona, W., and Maggio, R. D. (2010). Resistance of different types of concretes to cyclic sulfuric acid and sodium sulfate attack. *Cem. Concr. Compos.* 32, 595–602. doi:10.1016/j.cemconcomp.2010.07.002

Glasser, F. P., and Zhang, L. (2001). High-performance cement matrices based on calcium sulfoaluminate-belite compositions. *Cem. Concr. Res.* 31, 1881–1886. doi:10.1016/s0008-8846(01)00649-4

Gutiérrez-Padilla, M. G. D., Bielefeldt, A., Ovtchinnikov, S., Hernandez, M., and Silverstein, J. (2010). Biogenic sulfuric acid attack on different types of commercially produced concrete sewer pipes. *Cem. Concr. Res.* 40, 293–301. doi:10.1016/j.cemconres.2009.10.002

Hou, W., Liu, Z. Q., He, F. Q., Huang, J., and Zhou, J. (2020). Sulfate diffusion in calcium sulphoaluminate mortar. *Constr. Build. Mater.* 234, 117312. doi:10.1016/j.conbuildmat.2019.117312

Imbabi, M. S., Carrigan, C., and McKenna, S. (2012). Trends and developments in green cement and concrete technology. *Int. J. Sustain. Built Environ.* 1, 194–216. doi:10.1016/j.ijsbe.2013.05.001

Joorabchian, S. M. (2010). *Durability of concrete exposed to sulfuric acid attack*. Toronto: Ryerson University.

Kim, Y. Y., Lee, K. M., Bang, J. W., and Kwon, S. J. (2014). Effect of W/C ratio on durability and porosity in cement mortar with constant cement amount. *Adv. Mater. Sci. Eng.* 2014, 1–11. doi:10.1155/2014/273460

Larreur-Cayol, S., Bertron, A., and Escadeillas, G. (2011). Degradation of cement-based materials by various organic acids in agroindustrial waste-waters. *Cem. Concr. Res.* 41, 882–892. doi:10.1016/j.cemconres.2011.04.007

Li, H., Li, L., Li, L., Zhou, J., Mu, R., and Xu, M. (2022). Influence of fiber orientation on the microstructures of interfacial transition zones and pull-out behavior of steel fiber in cementitious composites. *Cem. Concr. Compos.* 128, 104459. doi:10.1016/j.cemconcomp.2022.104459

Li, J., Ma, B., Zhou, C., and Yang, Y. (2014). Study on mechanism of chemical activation for minerals of high belite-calcium sulfoaluminate clinker. *J. Sustain. Cement-Based Mater.* 3 (1), 13–23. doi:10.1080/21650373.2013.843476

Maddalena, R., Roberts, J. J., and Hamilton, A. (2018). Can Portland cement be replaced by low-carbon alternative materials? A study on the thermal properties and carbon emissions of innovative cements. *J. Clean. Prod.* 186, 933–942. doi:10.1016/j.jclepro.2018.02.138

Mlinárik, L., and Kopecskó, K. (2017). The influence of combined application of two SCMs on the corrosion and acid attack durability of mortars. *Period. Polytech. Civ. Eng.* 61 (2), 313–321. doi:10.3311/ppci.9352

Ninan, C. M., Ramaswamy, K. P., and Sajeeb, R. (2021). A critical review on the factors influencing the design of test methods for assessing acid attack in concrete. *IOP Conf. Ser. Mater. Sci. Eng.* 1114 (1), 012013. doi:10.1088/1757-899x/1114/1/012013

Ogawa, K., and Roy, D. M. (1982). C_4A_3S hydration, ettringite formation, and its expansion mechanism: III. Effect of CaO, NaOH and NaCl; conclusions. *Cem. Concr. Res.* 12, 247–256. doi:10.1016/0008-8846(82)90011-4

Que, Y., Dai, Y., Ji, X., Leung, A. K., Chen, Z., Tang, Y., et al. (2023). Automatic classification of asphalt pavement cracks using a novel integrated generative adversarial networks and improved VGG model. *Eng. Struct.* 277, 115406. doi:10.1016/j.engstruct.2022.115406

Sun, Z., Nie, S., Zhou, J., Li, H., Chen, Z., Xu, M., et al. (2022). Hydration mechanism of calcium sulfoaluminate-activated supersulfated cement. *J. Clean. Prod.* 333, 130094. doi:10.1016/j.jclepro.2021.130094

Wang, X., Guo, M., Yue, G., Li, Q., and Ling, T. C. (2022). Synthesis of high belite sulfoaluminate cement with high volume of mixed solid wastes. *Cem. Concr. Res.* 158, 106845. doi:10.1016/j.cemconres.2022.106845

Wu, H., Zhang, D., Du, T. J., and Li, V. C. (2020a). Durability of engineered cementitious composite exposed to acid mine drainage. *Cem. Concr. Compos.* 108, 103550. doi:10.1016/j.cemconcomp.2020.103550

Wu, M., Wang, T., Wu, K., and Kan, L. (2020b). Microbiologically induced corrosion of concrete in sewer structures: a review of the mechanisms and phenomena. *Constr. Build. Mater.* 239, 117813. doi:10.1016/j.conbuildmat.2019.117813

Wu, Z., Tang, Y., Hong, B., Liang, B., and Liu, Y. (2003). Enhanced precision in dam crack width measurement: leveraging advanced lightweight network identification for pixel-level accuracy. *Int. J. Intelligent Syst.* 2023, 9940881. doi:10.1155/2023/9940881

Xu, L. L., Wu, K., Li, N., Zhou, X. Y., and Wang, P. M. (2017). Utilization of flue gas desulfurization gypsum for producing calcium sulfoaluminate cement. *J. Clean. Prod.* 161, 803–811. doi:10.1016/j.jclepro.2017.05.055

Yang, Y., Ji, T., Lin, X. J., Chen, C. Y., and Yang, Z. X. (2018). Biogenic sulfuric acid corrosion resistance of new artificial reef concrete. *Constr. Build. Mater.* 158, 33–41. doi:10.1016/j.conbuildmat.2017.10.007

Yue, Q., Li, L., and He, Z. P. (2011). Experiment research on the steel fiber reinforced concrete in the acid environment. *Adv. Mater. Res.* 224, 224–228. doi:10.4028/www.scientific.net/amr.224.224

Zhang, W., Nie, S., Xu, M., Zhou, J., and Li, H. (2022). Research progress on activation of high belite calcium sulphoaluminate cement. *Bull. Chin. Ceram. Soc.* 41 (9), 2979–2992. doi:10.16552/j.cnki.issn1001-1625.2022.09.002

Zhang, Z. Q. (2015). *Rapid-setting and hardening, high-belite sulfoaluminate cement clinker as well as application and production process thereof*. US Patent 9822036B2.